Application, synthesis, isocyanate and polyol in underground seepage control engineering

Dengping Hu*[a,b,c], Chengchao Guo[a,b,c] and Xuanxuan Chu[d]

[a]School of Civil Engineering, [b]Guangdong Key Laboratory of Marine Civil Engineering,

[c]Guangdong Engineering Technology Research Center for Underground Space Development,
Sun Yat-sen University, Guangzhou 510275, China

[d]Nottingham Transportation Engineering Centre, Faculty of Engineering, University of Nottingham, University Park, Nottingham, NG7 2RD, United Kingdom

E-mail: hudengping668@163.com

The components of a waterproofing polymer are made up of isocyanate and polyol. The two components can react with each other, the isocyanate/polyol composite slurry expands rapidly after chemical reaction and solidifies immediately, a dense impermeable material was formed by rapid expansion of isocyanate and polyol, which is widely used for underground seepage control engineering. RNCO and R′OH react to form RNHCOOR′, RNCO reacts with water to produce RNHCONHR and carbon dioxide, the resulting carbon dioxide gas can promote the expansion of polymer materials. When carbon dioxide gas is produced, the reaction of two-component polymer will produce larger expansion force, as for the elastomer formed by the chemical reaction of the polymer, the expansion force peak value can reach more than 10 Mpa, gradually improving the crack resistance. At the same time, the composite material has good cementation with other structural materials after expansion. It will provide a good reference for specific engineering practice.

Keywords: Synthesis, isocyanate, polyol, seepage control engineering, dense impermeable material, carbon dioxide.

Introduction

Compared with the cement mortar grouting, the polymer grouting have many advantages, such as the early strength, convenient construction, grouting without water and non-shrinkage. When used in collapsible loess, expansive soil and various emergency maintenance, the advantages are more obvious.

In recent years, Shi Ming-sheng *et al*. creatively applied polymer grouting technology to geotechnical grouting engineering. Contrasting the polymer grouting with the ordinary mortar grouting in silt, they found that self-expanded properties of polymer remarkably increase the bonding strength between grouting body and hole wall, so grouting strength increases nearly twice as much as ordinary cement grouting. For 15 min after the reaction, strength materials can reach about 90%, without curing. That provides a type of new grouting technology for collapsible loess.

For some sandwiched composite structures, they can be composed of body core materials, e.g. polyurethane, which can form a good functional structure within some strong bonding structures[1]. For traditional polyurethane materials, they are featured by light weight, simple structure and higher strength than other materials. Besides, polyurethane polymer materials also include various types, e.g. corrugated sheets, nanomaterials, grid interlayer, honeycomb panels, lattice material and three-dimensional truss interlayer[2,3].

Currently, polyurethane composites have been widely promoted and utilized, and composite polymer high-performance materials have demonstrated excellent thermal stability, electrical conductivity and high strength. In terms of the above properties, polymer composites presented great development potential in many aspects[4–8]. The domestic and overseas researches mainly focused on adding carbon fiber into composite materials[9–15]. Compared with other new materials, this will indirectly reduce the density and affect the molecular particle size. Recently, there are some other studies

in the carbonaceous material added to the polyurethane[16–19]. For example, carbon black[20,21] can be gradually added to aqueous polyurethane materials, and in view of the fact that the molecular chain can also cause different physical properties of different polyurethane materials, more functional materials can now be made into polyurethane foam[22–24] and adhesive coatings, etc. Then, the products are employed for many different purposes of polyurethane products and plastic products and can also be widely used in construction[25,26], transportation and other industries.

In 1872, since the first usage of grouting in the slope of the open shale mine in North Welsh, UK, the development of geotechnical grouting technology has experienced a history of more than one hundred years. Since the 21st century, with the development of infrastructure, mining industry and underground engineering construction at home and abroad, geotechnical environments of grouting construction have become increasingly complex and diverse. New challenges arise in the grouting construction, so domestic and foreign experts and scholars concentrate on the researching of the new grouting materials and technology, which are perdurable, easy constructed and high strength[27].

Grouting has become one of the most economical and effective methods to improve the stability of soil-rock mass and solve the complex problems of underground engineering. Polymer grouting has been widely used in various fields of underground engineering, which relates to all aspects of engineering construction.

The research work for polymer grouting is roughly divided into three aspects, including developing polymer grouting of new structure, developing new bolt material and developing new anchorage grouting material. Based on developing a new type of grouting material, non-water reaction polymer grouting material used in underground engineering has been studied in this article.

In 1970s, the chemical solution composed of prepolymers of polyurethane foam started to be used for chemical grouting in geotechnical engineering (Naudts, 2003). However, the early polyurethane grout can't be applied to the environment without water, because their polymerization reaction needs the participation of water.

In the past two decades, the non-water reaction polyurethane polymer materials with expansile characteristics and their high pressure injection technique has developed rapidly. When such materials are injected into soil, rock mass or fissured or defected constructions, they react immediately and become polyurethane foam with their volume rapidly swelling and generating tremendous expanding power. With expanding force, they fill the voids, compact the surrounding medium, and block the leakage channel quickly.

For underground engineering purposes, it is of prime importance to understand the mechanical and hydro-mechanical behavior of such polymer grouting materials at solid state. Many relative studies have been documented over the past few years. Wang *et al.* (2011) investigated the anti-seepage properties of polyurethane foam referring to relevant concrete tests standards of China, and proposed a relationship curve between specimen density and initial seepage water pressure. Shi *et al.* (2010) experimentally examined the influence of temperature on compressive strength of polymer foam[28–32], and addressed that the compressive strength was not significantly affected by temperature when the density was less than 0.4 g/cm^3. Buzzi *et al.* (2008) studied the effect of heterogeneity on the mechanical and hydraulic properties of the polyurethane foam injected into ground[33], and proved that even though the heterogeneity led to an obvious reduction in yield stress and an increase in permeability, around 10^{-8} cm/s, it did not impair the validity of applying the expanding polymer foam in foundation remediation. Valentino (2014) established a relationship between the density of two polyurethane resins and the confinement pressure in expansion condition[34], and found an exponential relationship between the peak stress and resin density and between Young's modulus and resin density. However, little attention has been paid to polymer grout material's diffusion behavior in soil by now[35,36].

Generally, based on the above studies, a common conclusion has been drawn that the polymer material is a type of good grouting material with excellent comprehensive performances and extensive use in geotechnical engineering. It must be mentioned that in comparison with the current impervious material, e.g. clay slurry, cement slurry, reinforcement concrete and plastic concrete, the polyurethane foam is characterized by some prominent specialties, such as good crack resistance, light weight, without attaching additional

load to structure, curing rapidly and thus shortening the work period greatly.

Preliminary view that the polyurethane polymer material with expansion property has a compaction effect on the soil layer, which is beneficial to increase the friction force between the grout body and the matrix, polymer material of impermeability for the steel-made rods is impermeable material, which is advantageous to anticorrosion and durability of the rod body. The polymer material has great strength, which is conducive to improve the ultimate pullout force of single anchor, the solidification time of polymer materials is about 15~30 s requiring no maintenance, and it is advantageous to shorten the construction period. Based on the physical and mechanical properties of polyurethane polymer materials, it is feasible in theory to be used as grouting material in the anchoring technology.

The article may lay the foundation for further application of polymer grouting in underground environment engineering. But the applicability and feasibility of polymer grouting in underground engineering were also studied, to provide the technical basis for expanding the application of polymer grouting. Seepage is generally considered as a hidden danger threatening under the underground space project. The widely used impermeable materials at present, including clay grout, cement-based grout, plastic concrete and reinforced concrete, have significant shortcomings to different degrees. Compared with current impermeable materials, the polymer grout material exhibits potential advantages due to its excellent properties such as crack resistance, long durability, high early strenght, light weight, and so on.

Polymer grouting

It is the schematic diagram of polymer slurry, which is a dense impermeable material formed by rapid expansion of the interaction between isocyanate and polyol, as in Fig. 1. Grouting is carried out behind the steel panel[37], as shown Fig. 2(a)-(d), The polymer has good hydrophilicity, which will immediately undergo polymerization reaction upon contact with water, disperse, emulsify or foam and expand, quickly plug cracks and permanently stop water. The induction time can be controlled, and the consolidation time after the product meets water can be controlled in tens of seconds to sev-
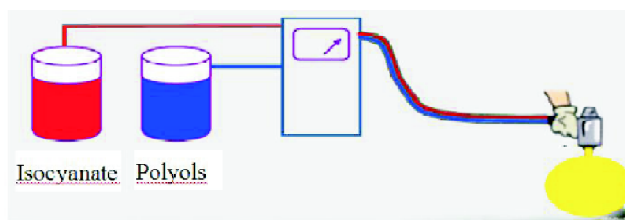

Fig. 1. Reaction of two-component high polymer.

(a) Grouting polymer

(b) Polymer layer is behind the steel panel

(c) Polymer grouting process

(d) Underground engineering

(e) Polymer grouting gun

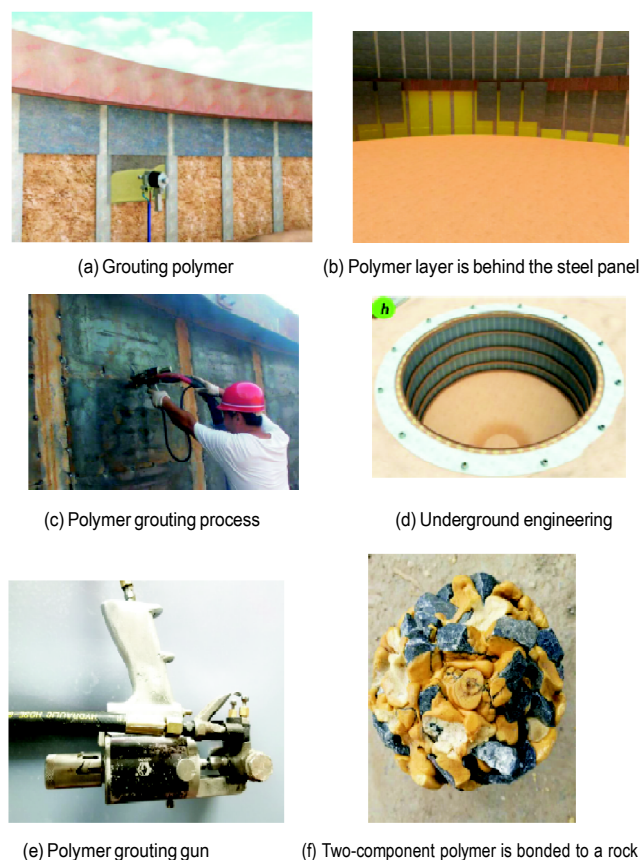(f) Two-component polymer is bonded to a rock

Fig. 2. Grouting behind the steel panel.

eral minutes. Large expansibility, good toughness, no shrinkage, strong adhesion to the substrate, and strong adaptability to water quality, good irrigation, even at low temperature can still be used for grouting. After grouting, a layer of impervious flexible polymer layer is formed betweem the steel panel and the soil. The polymer can be well bonded to the steel plate and exhibits good mechanical properties. The structure of the steel panel-polymer composite can play a good
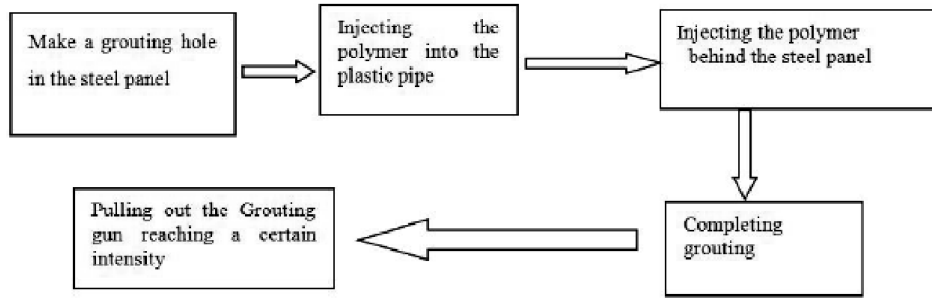
Fig. 3. The schematic of the grouting process.

coupling role. The adhesive force of high polymer is relatively large, polymer is bonded to a rock, grouting process is shown in Fig. 3, The polymer grouting material can be reacted with isocyanate and polyether polyols dehydrated at 110°C in a certain proportion at 80°C for 2 h, and then 10–30% diluent, 0.2–1% surfactant, 0.1–0.5% catalyst and 5–10% flame retardant are added. 36% of phosphorus-containing flame retardants, 15% of the physical foaming agent, 2% of the amine catalyst, another 1% of silicon surface active agent, 1% of the chemical foaming agent (water), the design is calculated according to the percentage.

Reaction of isocyanate with alcohol:

$$RNCO + R'OH \rightarrow RNHCOOR' \tag{1}$$

Reaction of isocyanate with water:

$$2RNCO + H_2O \rightarrow RNHCONHR + CO_2\uparrow \tag{2}$$

Polymer material tests

The main components of the polymer material are isocyanates and polyols. According to the study on the polymer, surface tension and surface energy existed at the interface of the vesicle. The surface energy increased with the surface area, whilst the stability of the system decreased, as in Fig. 4 and Fig. 5. The shape of the pores in the sample was spherical, under which the pores had the smallest specific surface area. The pores were far apart and did not interact with each other to ensure the minimum total surface energy of the system. The existing space was inadequate space to fill pores into a sphere, and then the pores would their sphericity and gradually became polyhedral with larger diameters, as in Figs. 6(a)-(d).
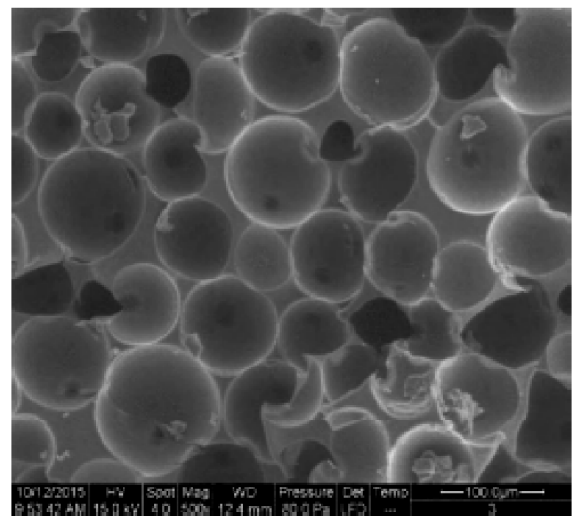

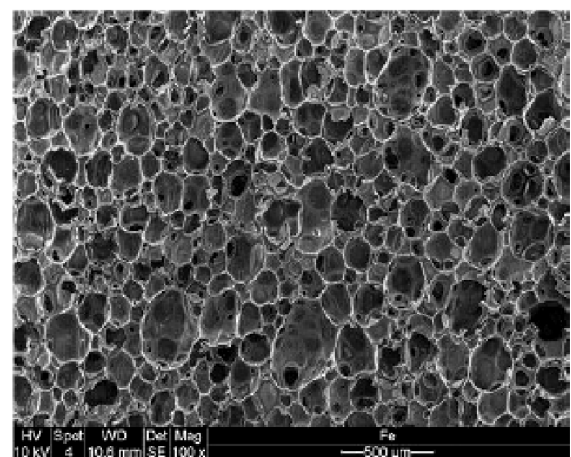**Fig. 4.** Scanning electron microscope of 100 um.

Fig. 5. Scanning electron microscope of 500 um.

(a) 50 um polymer microscopic image

(b) 50 um polymer magnifies image

(c) 200 um polymer image
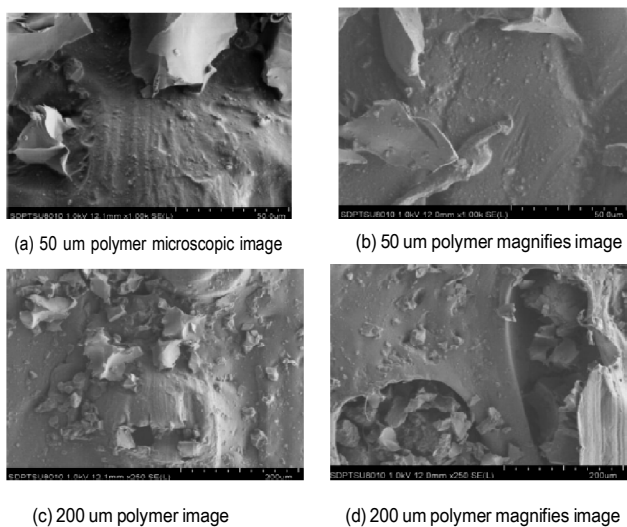

(d) 200 um polymer magnifies image

Fig. 6. Scanning electron microscope.

### The presence of acid base in polyurethane immersion

As can be seen from the Fig. 7(a)-(d), when polyurethane is soaked with hydrochloric acid and sulfuric acid, the internal spaces become smaller and the material becomes denser. Polyurethane is soaked with hydrochloric acid and sulfuric acid, the internal space of the material becomes smaller, the material becomes denser and has a better waterproof effect.

Polymer mechanical properties test

The plastic materials shear stress and shear deformation rate at any point are linear functions. According to the flow process of this fluid, the shear stress of the shear flow in

(a) Scanning electron microscopy of 50 um after immersion in hydrochloric acid
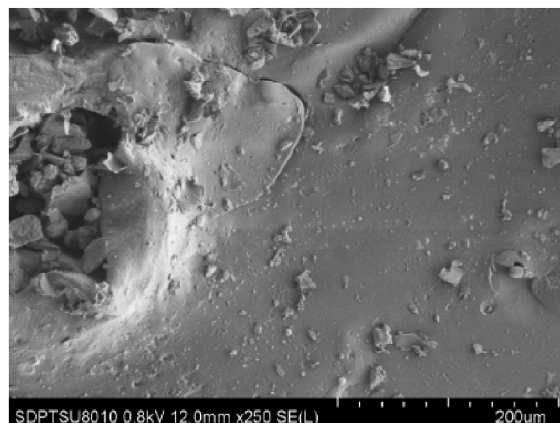
(b) Immersion hydrochloric acid scanning electron microscope 200 um
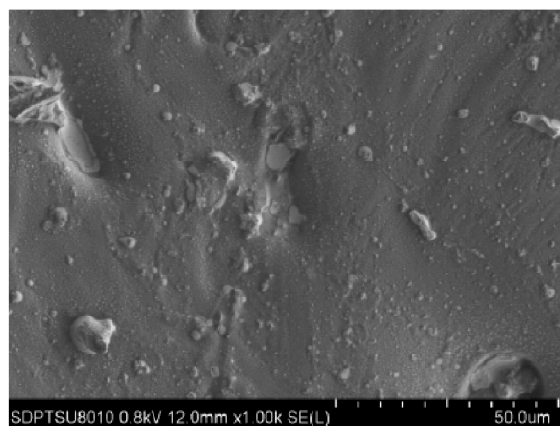
(c) Immersion sulfuric acid scanning electron microscope 50 um

(d) Immersion sulfuric acid scanning electron microscope 200 um

Fig. 7. The morphology of polymer under the action of acid and base.

the adjacent flow layer are proportional, as shown in Figs. 8(a)-(b). It shows the uniaxial compression of stress-strain
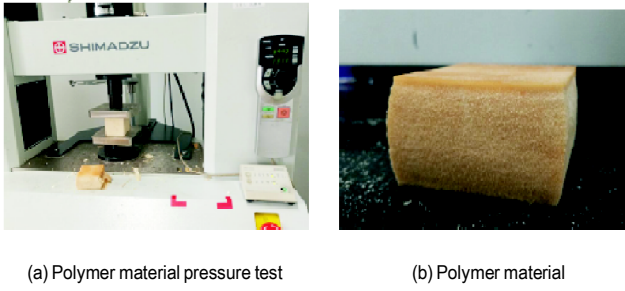
(a) Polymer material pressure test   (b) Polymer material

Fig. 8. Polymer material.

Fig. 10. Density analysis of polymer.

curves and morphology of polyurethane polymer samples with different densities after loading. During the application of uniaxial pressure, the response of the sample went through three stages: When the strain was less than 5%, it was in the elastic phase, and under small compressive stress, the bubble holes communicated with each other, and the irregular holes were firstly compressed into a regular sphere, which produced uniform deformation after compression. The edge of the bubble hole was caused by external force buckling[38,39]. The bubble busted, the material reached the yield strength, and the strain lay between 5% and 50%. As shown in Fig. 9 and Fig. 10.
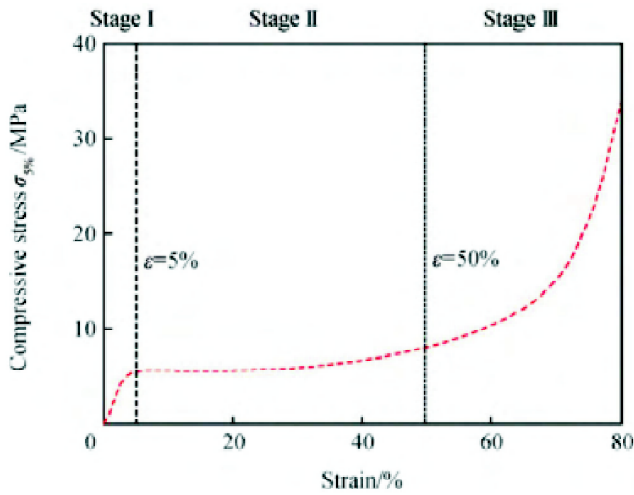

Fig. 9. Stress strain analysis of polymer.

Based on the specific properties of the polyurethane polymer composite, the constitutive model of the composite can
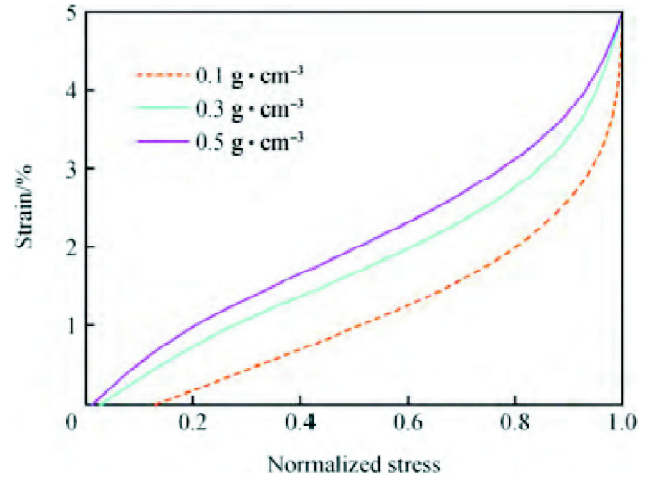
be determined. When the overall external force of the composite material is applied, it can be transferred to the next interface through the basic interface of the distributed load. Under a certain interface strength, the shear stress showed the largest value at the end of the material and the smallest value in the middle. The tensile stress acting on the composite derived from the cumulation of shear stress from the end to the middle. Thus, the tensile stress exhibited the smallest value at the end and the largest value at the middle. The material parameters and mechanical properties of the polyurethane polymer were continuously investigated. Based on the stress and deformation of the polymer materials, a stress-strain model can be established. σ represents the tensile stress in any direction, σ_{max} denotes maximum stress, $\bar{\sigma}$ is mean stress, l represents the composite fiber with a certain length, l_0 indicates the fundamental unit length of the composite material, β represents the composite material coefficient. According to the mechanical properties of the composite materials in different directions, it can be set that the orthotropic materials have three orthogonal planes, and the composite materials are denoted as orthotropic materials. For orthogonal anisotropic materials, the average tensile stress acting on the composite fiber is expressed as

$$\bar{\sigma} = \frac{1}{l}\int_0^l \sigma dl = \sigma_{max}\left[1-(1-\beta)\left(\frac{l_0}{l}\right)\right] \quad l \ge l_0 \qquad (3)$$

When the matrix of the composite material is an ideal plastic material, the tensile stress on the composite fiber gradually

increases from zero at the end of the material. When $\beta = 1/2$, eq. (3) can be expressed as

$$\bar{\sigma} = \sigma_{max}\left[1 - \frac{l_0}{2l}\right] \qquad (4)$$

If the matrix is an elastic material, eq. (3) can be rewritten as

$$\bar{\sigma} = \sigma_{max}\left\{\frac{1 - \sin^{-1}\tanh\left[A(l/d)\right]}{A(l/d)}\right\}, \qquad (5)$$

$$A = \frac{24(G_1/E_1)[1 + (V_1/V_2)(E_1/E_2)]}{1 - 3(G_1/G_2) + 2G_1/G_2(V_1^{-2/3} - 1)(V_1^{-1} - 1)} \qquad (6)$$

where G_1 and G_2 represent shear moduli in orthogonal directions respectively, E_1 and E_2 represent Young's moduli in the orthogonal directions, V_1 and V_2 are the Poisson's ratio in the orthogonal directions, h denotes varying height, d represents the diameter of composite fiber. The relationship between matrix yield strength and composite material dimension can be described as

$$\frac{l}{d} = \frac{\sigma_{max}}{2\tau_{max}} \qquad (7)$$

where τ_{max} is the yield strength of the matrix.

Then, the tensile strength of the short fiber reinforced composite is:

$$\sigma_F = \sigma\left(1 - \frac{l_x}{2l_y}\right)V_1 + \sigma_m(1 - V_1) \qquad (8)$$

where τ_F is the average tensile stress of composite fiber, l_x and l_y are the matrix elements representing orthogonal directions. The tensile strength of the composite material in the x direction increased with $\frac{l_x}{l_y}$.
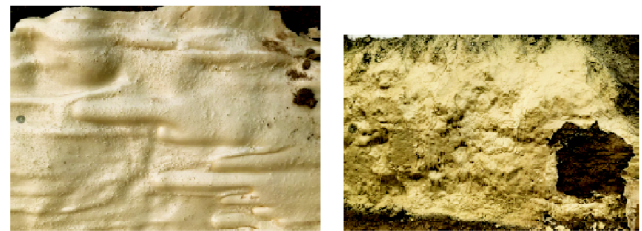
The polymer is bonded to the steel panel

The original length range is 1250 mm in the length direction, and the original rule in the height direction is called 560 mm. The bond between the steel panel and the polymer is shown Fig. 11 composite structure to ensure that the steel plate and the side soil are tightly bonded to the wall. After injecting the steel sheet, a thin layer polymer structure having a certain strength is formed, which can play the role of

Fig. 11. Polymer bonded steel panel.

waterproofing and deformation resistance, and has great engineering application potential, the polymer is bonded to the earth wall, as shown in Fig. 12(a)-(b). Adhesion between steel panel and polymer density increases with increased significantly, and when the polymer body density greater than 0.4 g/cm^3. The bonding force between the polymer and the steel panel increases gradually; with the increase of polymer density, the bonding force between the polymer and the steel panel increases gradually. Polymer grouting body can form impervious curtain after soil mass. It has a good effect of preventing soil deformation. The two materials can be mixed to a certain proportion. The polymer of two components can expand after reaction, it has a good effect of preventing soil deformation.

(a) Polymer impermeable waterproof layer   (b) The polymer is bonded to the soil

Fig. 12. The steel panel is bonded to the earth wall.

Bonding strength refers to the strength generated by the relative sliding resistance on the contact surface between the polymer grouting body and the steel panel, which is an indicator characterizing the adhesive properties between the grouting body and the steel panel, usually expressed in the average bond strength. Although there are large differences

Table 1. The material parameter table

Parameter material	Density (kg/m^3)	Young modulus (N/m^2)	Poisson's ratio (°)	Frictional angle (°)	Expansion angle (KPa)	Cohesive force
Soil mass	1800	1×10^7	0.3	23.05	17.83	45.92
Polymer	200~600	–	0.3	–	–	–
Steel panel	7850	2×10^{11}	0.3	–	–	–

in the physical and mechanical properties between polymer grouting body and cement mortar grouting body, but the formation mechanisms of the bonding strength are similar. Reference to the formation mechanism of bonding strength of cement mortar grouting body, can infer the bonding strength of polymer grouting body is mainly composed of the following three components, as shown in Table 1 for parameters.

The polymer is bonded to the steel panel

As can be seen bonding strength refers to the strength generated by the relative sliding resistance on the contact surface between the polymer grouting body and the steel panel, which is an indicator characterizing the adhesive properties between the grouting body and the steel panel, usually expressed in the average bond strength. Although there are large differences in the physical and mechanical properties between polymer grouting body and cement mortar grouting body, but the formation mechanisms of the bonding strength are similar. Reference to the formation mechanism of bonding strength of cement mortar grouting body, can infer the bonding strength of polymer grouting body is mainly composed of the following three components, as shown Table 1 for parameters.

Conclusion

The isocyanate/polyol composite slurry expands rapidly after chemical reaction and solidifies immediately, a dense impermeable material was formed by rapid expansion of isocyanate and polyol, which is widely used for underground seepage control engineering. When carbon dioxide gas is produced, the reaction of two-component polymer will produce larger expansion force, as for the elastomer formed by the chemical reaction of the polymer.

(i) Chemical cementing force on the interface between polymer grouting body and surface of the other material structures. Since the polymeric material itself has a certain cementing force, the interface will produce cementing force,

which belongs to adsorption of different materials. Once the polymer and other material structures generate slippage, this force will immediately disappear and no longer be recovered.

(ii) Friction of the polymeric material and the surface of the other material structures. Both polymer grouting body and the surface of the other material structures are rough surface, so the contact surface when drawn is bound to produce friction. The size of the friction depends on the friction coefficient of the polymer and the other material structures, as well as the normal stress of the grouting.

(iii) which produce interlocking and greatly improve the bonding strength. Due to the strength of the other material structures material is generally higher than the strength of the grouting material, so the mechanical interlocking will disappear until the polymer material in the concave is damaged, and its ultimate value is determined by the shear strength and tensile strength of polymer materials.

References

1. A. P. Mouritz, E. Gellert, P. Burchhill and K. Challis, *Compos. Struct.*, 2001, **53**, 21.
2. Q. H. Cheng, H. P. Lee and C. Lu., *Compos. Struct.,* 2006, **74**, 226.
3. D. Y. Seong, C. G. Jung, D. Y. Yang, K. J. Moon and D. G. Ahn, *Mater. Design.,* 2010, **31**, 2804.
4. T. Gong, A. A. Heravi, G. Alsous, I. Curosu and V. Mechtcherine, *Appl. Sci-basel*, 2019, **9**, 4048.
5. Q. H. Cheng, H. P. Lee and C. Lu., *Compos. Struct.*, 2006, **74**, 226.
6. C. C. Guo, B. Sun, D. P. Hu, F. M. Wang, M. S. Shi and X. L. Li, *Soil Mech. Found. Eng.*, 2019, **86**, 171.
7. J. M. Martín-Martínez, T. G. Maciá-Agullo, J. C. Fernández-García, A. C. Orgiles-Barceló and A. Torró-Palau, *Macromo-*

lecular Symposia, 1996, **108**, 269.

8. L. Jiang, Y. C. Lam, K. C. Tam, D. T. Li and J. Zhang, *Polym. Bull.,* 1996, **57**, 575.

9. Á. Sonia and M. M. José, *J. Adhes. Sci. Technol.*, 2015, **29**, 1136.

10. I. S. Gunes, G. A. Jimenez and S. C. Jana, *Carbon*, 2009, **47**, 981.

11. S. A. Abdullah, A. Iqbal and L. Frormann, *J. Appl. Polym. Sci.,* 2008, **110**, 196.

12. J. P. Adohi, A. Mdarhri, C. Prunier, B. Haida and C. Brosseau, *J. Appl. Phys.*, 2010, **108**, 074108.

13. M. M. Rahman, E. Y. Kim, K. T. Lim and W. K. Lee, *J. Adhes. Sci. Technol.*, 2009, **23**, 839.

14. M. Fernández, M. Landa, M. A. Muñoz and A. Santamaria, *Macromol. Mater. Eng.*, 2010, **295**, 1031.

15. G. L. Burkholder, Y. W. Kwon and R. D. Pollak, *J. Mater. Sci.*, 2011, **46**, 3370.

16. F. Li, L. Qi, J. Yang, X. Luo and X. Ma, *J. Appl. Polym. Sci.*, 2000, **75**, 68.

17. M. Kozlowski, *Polym. Networks Blends*, 1995. **5**, 163.

18. K. C. Kil, G. Y. Kim, C. W. Cho, M. D. Lim, K. Kim, K.-M. Jeong, J. Lee and U. Paik, *Electrochim. Acta*, 2013, **111**, 946.

19. E. Andreoli, K. S. Liao, A. Cricini, X. Zhang, R. Soffiatti, H. J. Byrne and S. A. Curra, *Thin Solid Films*, 2014, **550**, 558.

20. Y. F. Du, P. W. Shi, Q. Y. Li, Y. C. Li and C. F. Wu, *Colloid Surface A*, 2014. **454**, 1.

21. J. Donate-Robles, C. M. Liauw, Martín-Martínez and José Miguel, *Int. J. Adhes. Adhes.*, 2014, **48**, 43.

22. X. Lan, W. Huang and J. Leng, *Appl. Sci-basel*, 2019 **9**, 2919.

23. D. K. Chattopadhyay and K. V. S. N. Raju, *Prog. Polym.*

24. K. Shimizu, M. L. Abel and C. Phanopoulos, *J. Mater. Sci.*, 2012, **47**, 902.

25. D. V. Palaskar, Aurélie Boyer and E. Cloutet, *et al., J. Polym. Sci. Pol. Chem.,* 2012, **50**, 1766.

26. H. Beneš, J. Rösner and P. Holler, *Polym. Advan. Technol.*, 2007, **18**, 149.

27. Shi Ming-sheng, *et al., China Harbour Engineering*, 2011, **3**.

28. Guo Cheng-chao, Wang Fu-ming and Xu Jian-guo, *Road Machinery & Construction Mechanization*, 2008, **25**, 60.

29. Guo Cheng-chao, Wang Fu-ming, 2009, GeoHunan International Conference (GSP191):110(2009).

30. Shi Ming-sheng, *et al., Chinese Journal of Geotechnical Engineering*, 2014, **4**, 724.

31. Guo Cheng-chao, Ph.D. Thesis for Dalian University of Technology, 2012.

32. Alex Naudts, ASCE Publications, Proceedings of 3nd International Specialty Conference on Grouting and Ground Treatment, New Orleans, USD, 2003, 1266.

33. O. Buzzi, S. Fityus and S. Sloan, *Can. Geotech. J.*, 2010, **47**, 623.

34. R. Valentino, E. Romeo and A. Misra, *Geotech. Geol. Eng.*, 2013, **31**, 463.

35. O. Buzzi, S. Fityus, Y. Sasaki and S. Sloan, *Mech. Mater.*, 2008, **40**, 1012.

36. R. Valentino a, E. Romeo a and D. Stevanoni, *Mech. Mater.*, 2014, **71**, 101.

37. Y. Pan, H. Fang, B. Li and F. Wang, *Eng. Struct.*, 2019, **192**, 205.

38. X. Gao, Y. Wei, F. Wang and Y. Zhong, *Acta Materiae Compositae Sinica*, 2017, **34**, 550.

39. X. Gao, H. Wei, W. Ya and Y. Zhong, *Acta Materiae Compositae Sinica*, 2017, **34**, 438.